

## SUPPORTING INFORMATION

### Highly Sensitive and Rapid Detection of Hypochlorous Acid in Aqueous Media and its Bioimaging in Live Cells and Zebrafish using ESIPT-Driven Mycophenolic Acid-Based Fluorescent Probe

Prasad M. Sonawane<sup>a</sup> †, Neha Jain<sup>a</sup> †, Arkaprava Roychaudhury<sup>b</sup> †, Su Jeong Park<sup>c</sup> †, Vikas K. Bhosale<sup>a</sup>, Mahesh B. Halle<sup>a</sup>, Cheol-Hee Kim<sup>b,\*</sup>, Satish Balasaheb Nimse<sup>c,\*</sup> and David. G. Churchill<sup>a, d\*</sup>

<sup>a</sup>*Department of Chemistry, Molecular Logic Gate Laboratory, Korea Advanced Institute of Science and Technology (KAIST), Daejeon, 34141, Republic of Korea.*

<sup>b</sup>*Department of Biology, Chungnam National University, Daejeon 34134, Republic of Korea.*

<sup>c</sup>*Institute of Applied Chemistry and Department of Chemistry, Hallym University, Chuncheon 24252, Republic of Korea.*

<sup>d</sup>*KAIST Institute for Health Science and Technology (KIHST) (Therapeutic Bioengineering Section), 291 Daehak-ro, Yuseong-gu, Daejeon 34141, Republic of Korea.*

\*Corresponding authors.

**Email address:** [zebrakim@cnu.ac.kr](mailto:zebrakim@cnu.ac.kr) (C. H. Kim),

[satish\\_nimse@hallym.ac.kr](mailto:satish_nimse@hallym.ac.kr) (S.B.N.)

[dchurchill@kaist.ac.kr](mailto:dchurchill@kaist.ac.kr) (D. G. Churchill)

# Table of contents

❖ General information	S3–S4.
❖ Table S1. The summary of previously reported fluorescent probes for the detection of HOCl	S5–S7.
❖ Synthesis	S8.
❖ Proposed sensing mechanism of Myco-OCI with OCI <sup>-</sup>	S8–S9.
❖ <sup>1</sup> H NMR spectra, 2D spectra, IR and HR–MS spectra	S10– S14.
❖ Photophysical study	S15–S17.
❖ Cell imaging study	S18.
❖ Zebrafish imaging study	S18–19.
❖ Additional references	S20.

## General Information:

*Reagents:* All chemicals used for experimental procedures were purchased from commercial suppliers like Sigma–Aldrich, Tokyo Chemical Industry, etc. Unless noted, all the chemicals used were of pure analytical reagent grade and used, as such, without any further purification or other treatment. Solvents such as dichloromethane, and N, N–dimethylformamide (DMF) were distilled from calcium hydride. All reaction conditions were performed by well–oven–dried apparatus components while being held under an N<sub>2</sub> blanket. When performing experiments, all air and moisture–sensitive compounds were introduced via syringe. Performance and progress of the reactions were observed by thin-layer chromatography (TLC). All components were purified by flash column chromatography by using E. Merck silica gel 60 (230–400 mesh ASTM).

*Instruments:* All mentioned below Nuclear magnetic resonance (NMR) spectra were measured on an Agilent–NMR– 400 MHz spectrometer. ESI–mass spectrometry was recorded on a BRUKER micro OTOF–QII. A Time–of–Flight mass spectrometer was operated at a resolution of 20,000. The fluorescence spectra were measured and recorded using a Shimadzu RF–5301pc spectrofluorophotometer and the absorption spectra were collected using a JASCO V–530 spectrophotometer.

## Experimental

### Generation of Different ROS and RNS Species

**Generation of OCl<sup>-</sup>:** HOCl solutions were prepared by using commercially available NaOCl bleach; its concentration was determined by measuring the absorbance at 209 nm (molar extinction coefficient = 350 M<sup>-1</sup>cm<sup>-1</sup>).

**Generation of H<sub>2</sub>O<sub>2</sub>:** Hydrogen peroxide (H<sub>2</sub>O<sub>2</sub>) solution was directly prepared by commercially available 30% H<sub>2</sub>O<sub>2</sub> solution; its concentration was determined by measuring the absorbance at 240 nm with a molar extinction coefficient of 43.6 M<sup>-1</sup> cm<sup>-1</sup>.

**Generation of <sup>t</sup>BuOOH:** The tert–butyl hydroperoxide solutions were formed through dilution with deionized water and stirred well before use.

**Generation of O<sub>2</sub><sup>-•</sup>:** Potassium superoxide (KO<sub>2</sub>) was dissolved in DMSO and stirred well before use<sup>1,2</sup>. The solution was used immediately.

**Generation of •OH:** Hydroxyl radical (•OH) was produced by the Fenton-type reaction *in situ*. Ferrous chloride (FeCl<sub>2</sub>) was added to 10 equiv. of hydrogen peroxide to help generate the hydroxyl radical.

**Generation of peroxynitrite (ONOO<sup>-</sup>):** To a precooled mixture of NaNO<sub>2</sub> and H<sub>2</sub>O<sub>2</sub>, hydrochloric acid followed by NaOH was added quickly. This stock solution was placed at temperatures lower than –18 °C.

The solution was always brought to ambient temperature and used directly. To determine the concentration of the stock solution, it was dissolved in 0.10 M NaOH and measured the absorbance at 302 nm with a molar extinction coefficient of 1670 M<sup>-1</sup>cm<sup>-1</sup>.

**Generation of NO•:** Nitric oxide was produced from SNP (sodium nitroferricyanide (III) dehydrate). All experiments were executed under anaerobic conditions. Initially, the deionized water was degassed well with argon for about 60 min; then finally, SNP was mixed into degassed and deionized water under an argon blanket and further stirred (well) for about 30 min at ambient temperature. Before the reaction of NO• with the molecular probe, this analyte solution was also degassed well with argon.

### Determination of the detection limit

The detection limit (LOD) was calculated based on fluorescence titrations. To achieve the standard deviation ( $\sigma$ ) of the blank measurement, fluorescence emission spectra of the probe **Myco-OCI** were measured three times in the absence of <sup>-</sup>OCI. Specifically, to obtain the value of the slope (k), the fluorescence intensity at 522 nm was plotted as a concentration of <sup>-</sup>OCI. Finally, LOD was calculated with the following equation:

$$\text{Detection limit} = 3\sigma/k$$

Where  $\sigma$  is the standard deviation of 10 blank measurements, k is the slope of the calibration curve and 3 is used as a calibration of signal-to-noise ratio.

All data were taken in PBS (10 mM) buffer solution of pH = 7.4 and incubated for 1 min.

### Determination of the Quantum Yield

$$\Phi_1 = \frac{\Phi_B I_1 A_B \lambda_{exB} \eta_1}{I_B A_1 \lambda_{ex1} \eta_B}$$

Where  $\Phi$  is the fluorescence quantum yield

I is the integrated area under the corrected emission spectral signal

A is the absorbance at the excitation wavelength

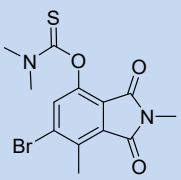
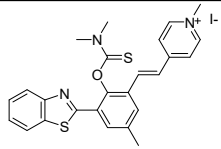
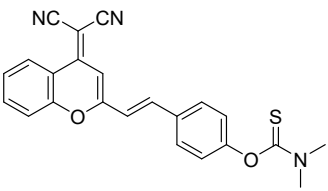
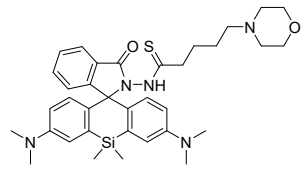
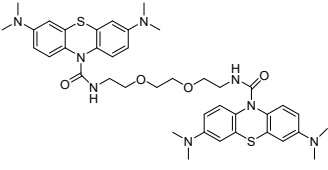
$\lambda_{ex}$  is the excitation wavelength

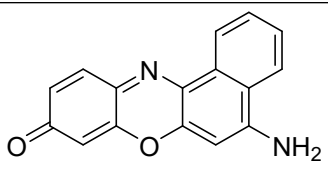
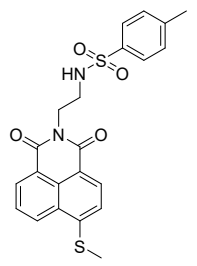
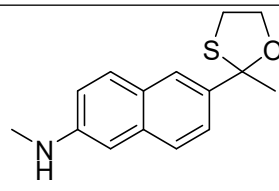
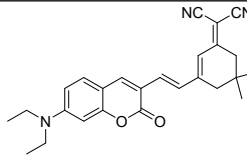
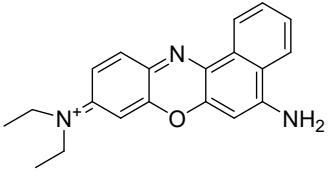
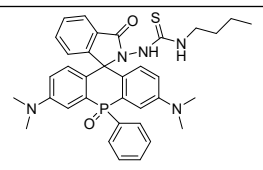
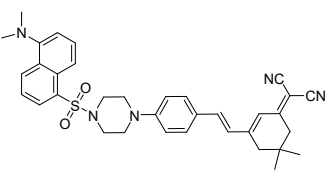
$\eta$  is the refractive index of the solution

The subscripts 1 and B refer to the unknown and the standard, respectively.

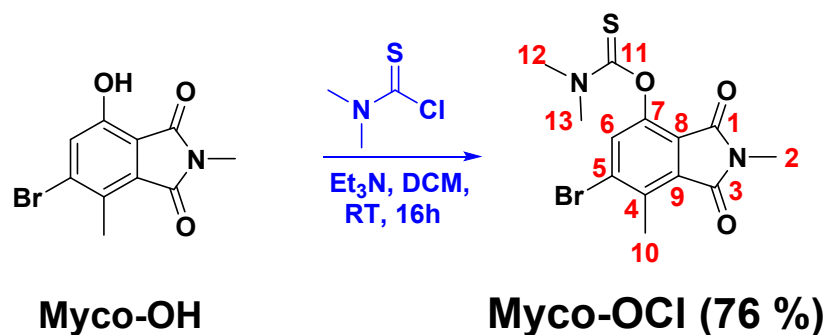
We chose the fluorescein standard which is present with 0.10 M NaOH as standard additive. Under these conditions, the quantum yield of this species is 0.95.

**Table S1.** The summary of previously reported fluorescent probes for the detection of HOCl.

Probes	Stokes Shift (nm)	LOD	Response time	Solvent	Bio-Applications	Ref.
	105	97.33 nM	< 5 s	PBS	Cells Zebrafish	This work
	170	0.47 μM	4 s	MeOH: water 1: 4 v/v	Cells Mice	Chem. Sci. 2019, 10, 3715-3722.
	140	164 nM	5 min	50% DMSO/ 10 mM PBS (7.4)	Cells	Talanta 2019, 196, 352-356.
	60	20 nM	10 min	50% DMSO/ 10 mM PBS (5)	Cells Mice	Anal. Chim. Acta. 2018, 1048, 143- 153.
	< 30 nm	31.7 nM	< 30 s	1% DMF/ 10 mM PBS(7.4)	Cells <i>C. elegans</i>	Dyes Pigm. 2020, 177, 108308.

	46	72 nM	10 min	10 mM PBS(7.4)	Cells	Talanta 2020, 215, 120892
	109	120 nM	< 3 min	1.0% DMSO 10 mM PBS(7.4)	Cells Zebrafish	Spectrochim. Acta. Part A: Mol. Biomol. Spectrosc. 229, 117992, (2020)
	125	16.6 nM	Within seconds	50% EtOH PBS(7.4)	Cells Mice	J. Am. Chem. Soc.2015, 137, 5930.
	155	0.17 μM	100 s	30% EtOH/PBS	Cells Mice	Sens. Actuators B 2019, 287, 453- 458.
	37	10.8 pM	< 5 s	PBS (0.01 M, pH = 7.4)	Cells	Biosens. Bioelectron. 2018, 107, 218–223.
	20	20 nM	20 s	PBS (pH = 7.4)	Cells Mice	Sens. Actuators B 2020, 307, 127652.
	300 pseudo Stokes shift	0.19 μM	25 s	DMF: PBS (5: 5, v/v; pH = 7.4)	Cells	Sens. Actuators B 2018, 255, 666– 671.

## 1. Synthesis



### Synthesis of Myco-OCl.

The Myco-OH was prepared by literature methods.<sup>21</sup>

Myco-OH (62.5 mg, 0.2 mmol) was dissolved in anhydrous DCM (5 ml) in the N<sub>2</sub> environment and stirred for 5 minutes. Then, this solution was treated with triethylamine (56  $\mu$ L, 0.6 mmol) and stirred again for 15 minutes to afford a clear solution. After that, dimethylthiocarbamoyl chloride (37 mg, 3.00 mmol) was added slowly at 0°C. This mixture was stirred for 16 h at room temperature. The solvent was evaporated and the residue was purified by silica gel flash chromatography using n-hexane/EtOAc (16:1) as an eluent to afford **Myco-OCl** as a white solid (97 mg, 76% yield). <sup>1</sup>H NMR (400 MHz, DMSO-d<sub>6</sub>):  $\delta$  = 7.85 (s, 1H, H<sub>6</sub>), 3.38 (s, 3H, H<sub>2</sub>), 3.37 (s, 3H, H<sub>13</sub>), 2.98 (s, 3H, H<sub>12</sub>), 2.67 (s, 3H, H<sub>10</sub>). <sup>13</sup>C NMR (100 MHz, DMSO-d<sub>6</sub>)  $\delta$ : 185.52 (C<sub>11</sub>), 167.77 (C<sub>3</sub>), 164.98 (C<sub>1</sub>), 147.60 (C<sub>7</sub>), 135.05 (C<sub>9</sub>), 133.63 (C<sub>8</sub>), 131.91 (C<sub>5</sub>), 130.73 (C<sub>4</sub>), 123.39 (C<sub>6</sub>), 43.49 (C<sub>12</sub>), 39.31 (C<sub>13</sub>), 24.26 (C<sub>2</sub>), 16.84 (C<sub>10</sub>). HRMS (ESI): calcd for C<sub>13</sub>H<sub>13</sub>BrN<sub>2</sub>O<sub>3</sub>S + Na: 380.9832; found:  $m/z$  380.9706 (M + Na)<sup>+</sup>.

### Proposed sensing mechanism:

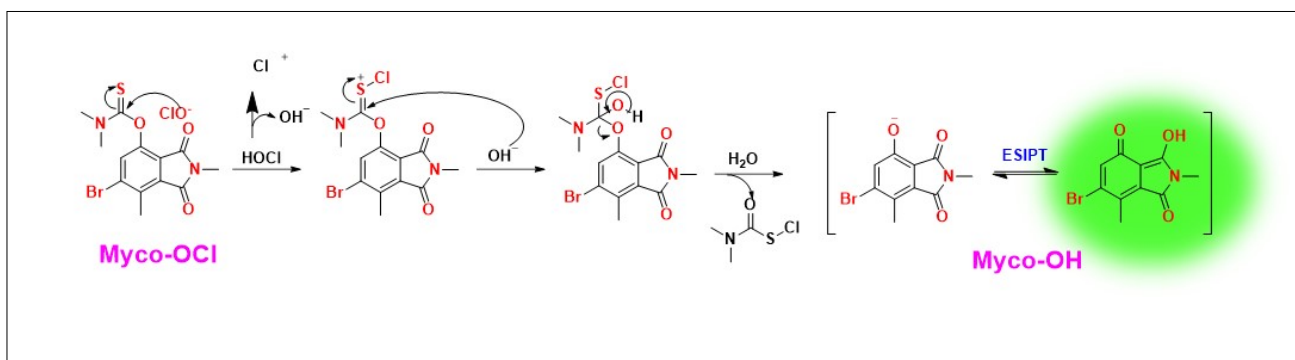
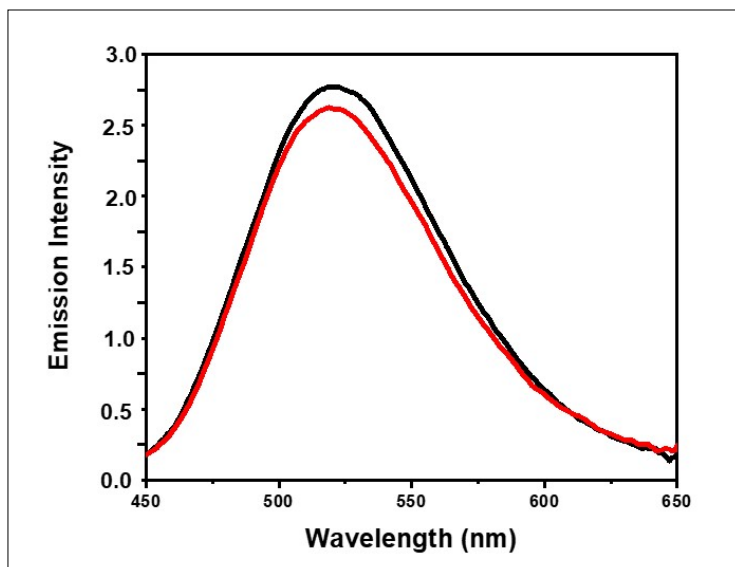
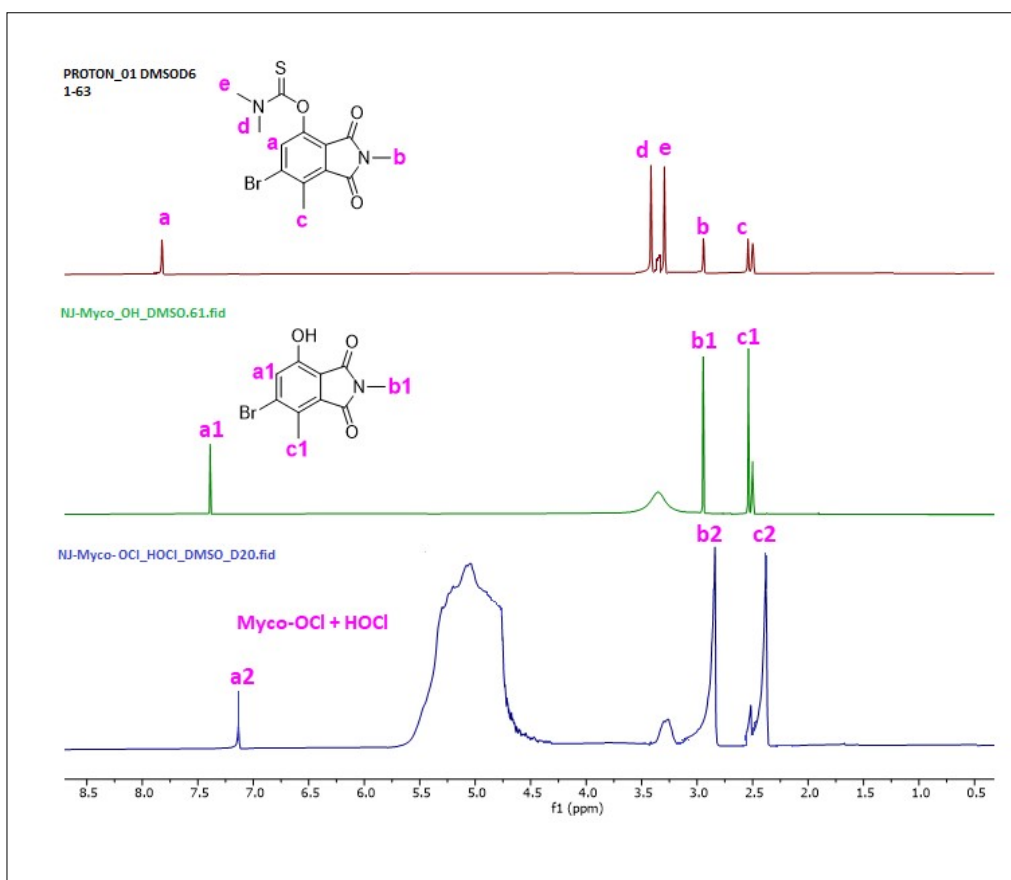


Fig. S1. Proposed sensing mechanism of HOCl with probe Myco-OCl<sup>3</sup>.



**Figure S2.** Normalize Emission spectra for the comparison between the probe **Myco-OCl** (red line) in response to HOCl (5 Eq.) and the fluorophore **Myco-OH** (black line).



**Fig. S3.**  $^1\text{H}$  NMR spectrum of the **Myco-OCl** in  $\text{DMSO-d}_6$  (brown line),  $^1\text{H}$  NMR spectrum of the **Myco-OH** in  $\text{DMSO-d}_6$  (green line), and  $^1\text{H}$  NMR spectrum of the **Myco-OCl + HOCl** (5 Eq.) (Blue line) in  $\text{DMSO-d}_6$  and  $\text{D}_2\text{O}$ .



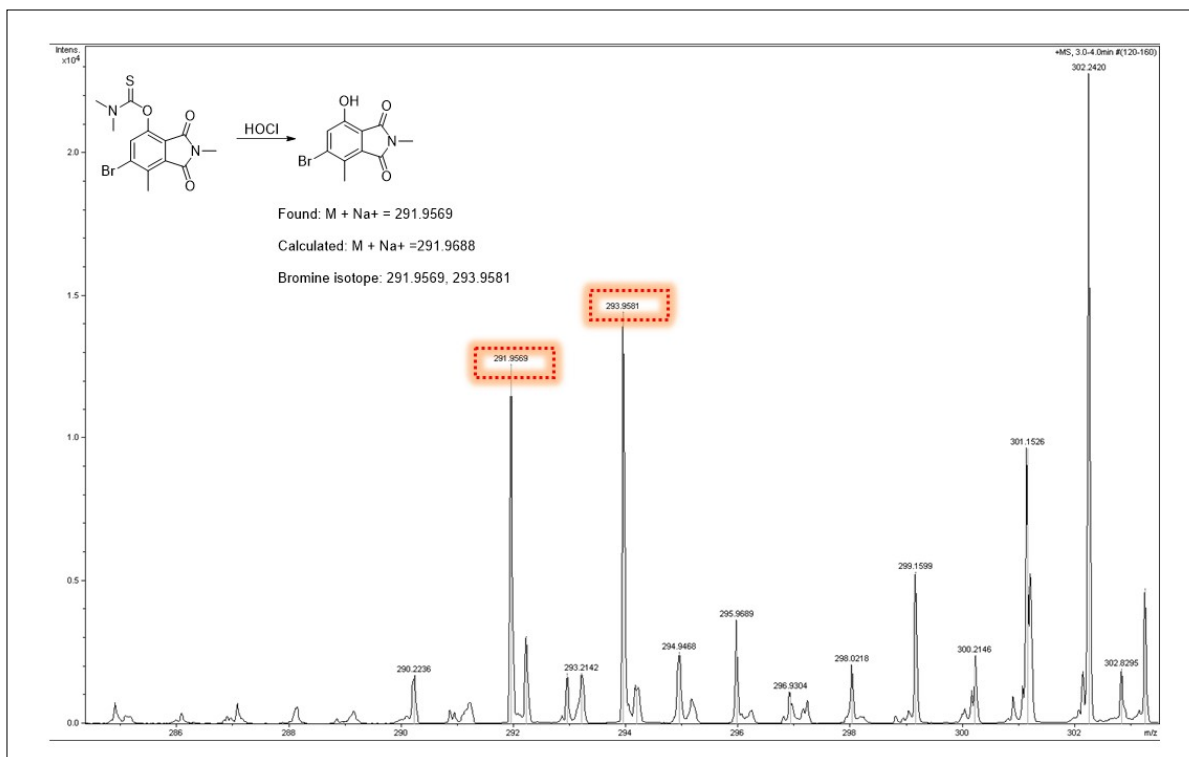


**Fig. S4.** HR-MS (ESI) spectrum of Myco-OCI + HOCl.

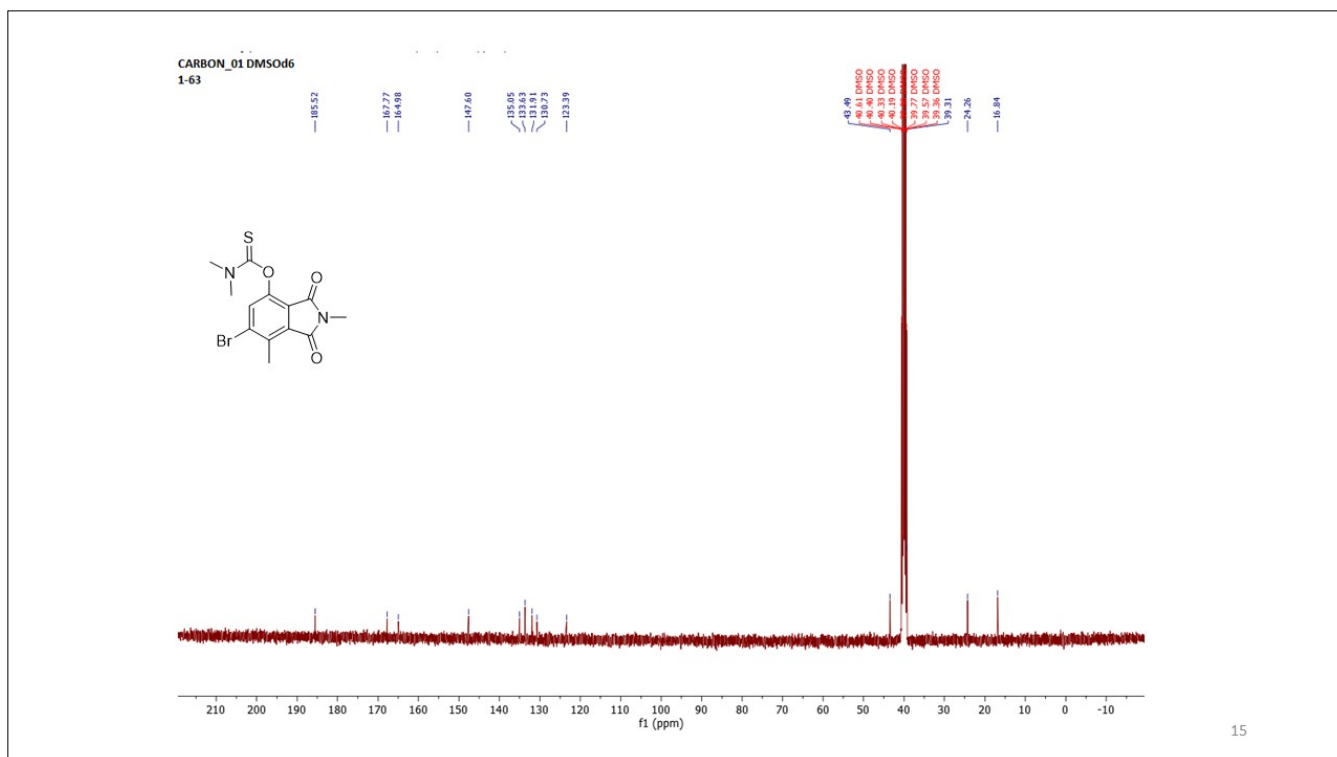
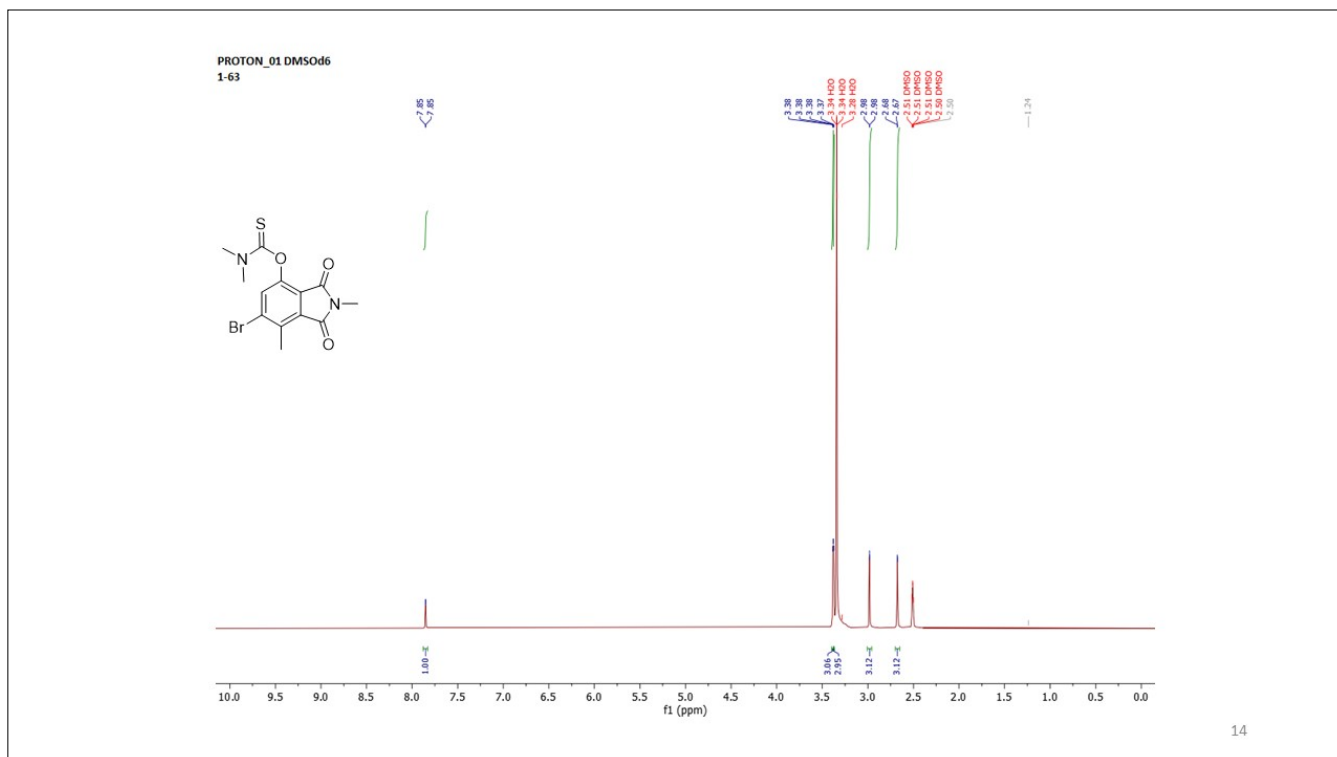


Fig. S5. (top) <sup>1</sup>H and (bottom) <sup>13</sup>C NMR spectrum of Myco-OCl.

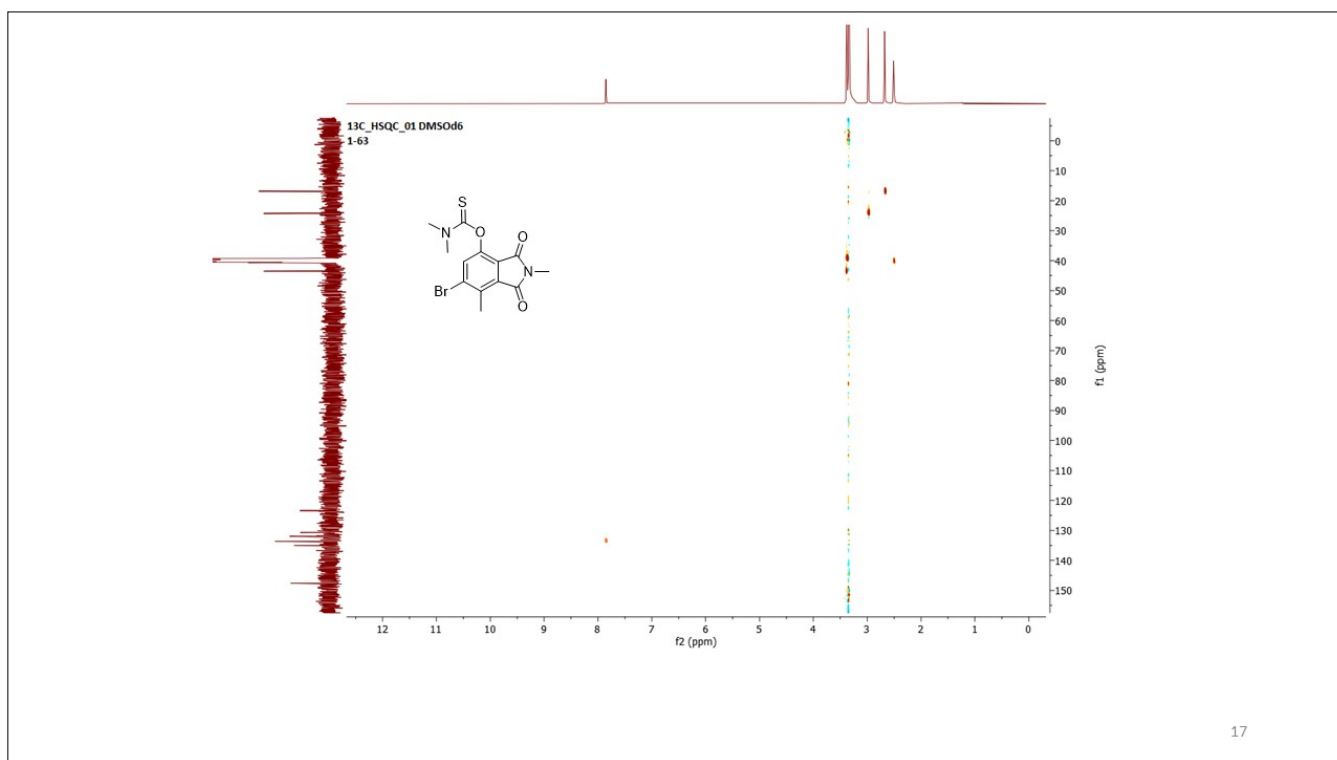
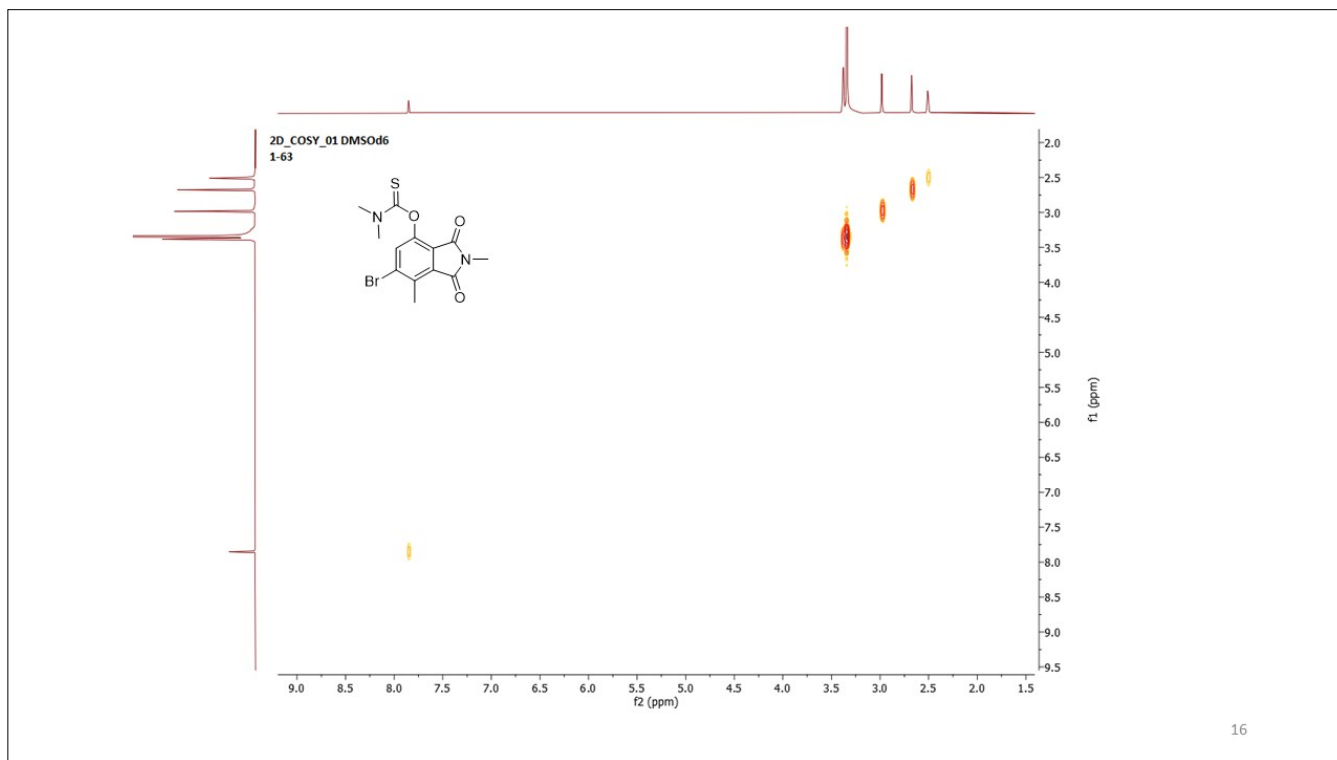


Fig. S6. (top) COSY spectrum and (bottom) HSQC NMR spectrum of **Myco-OCl**.

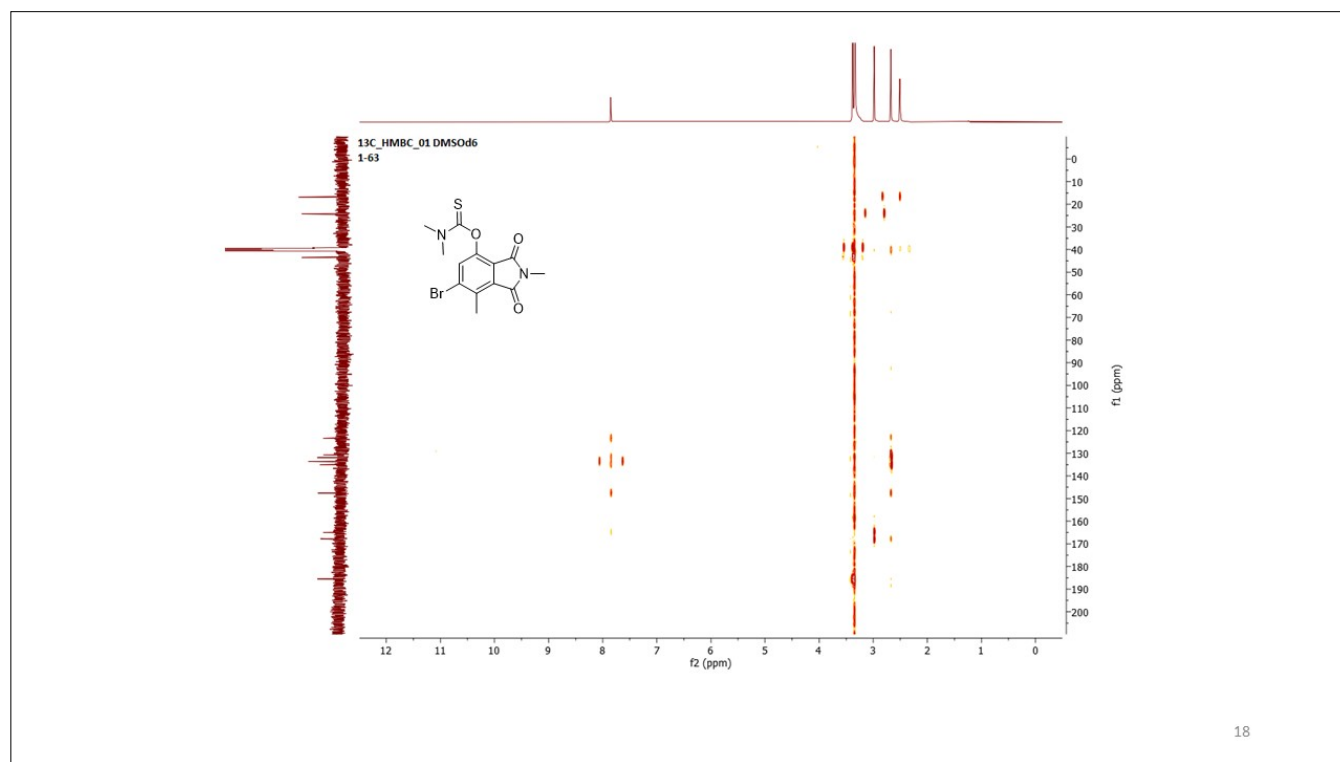
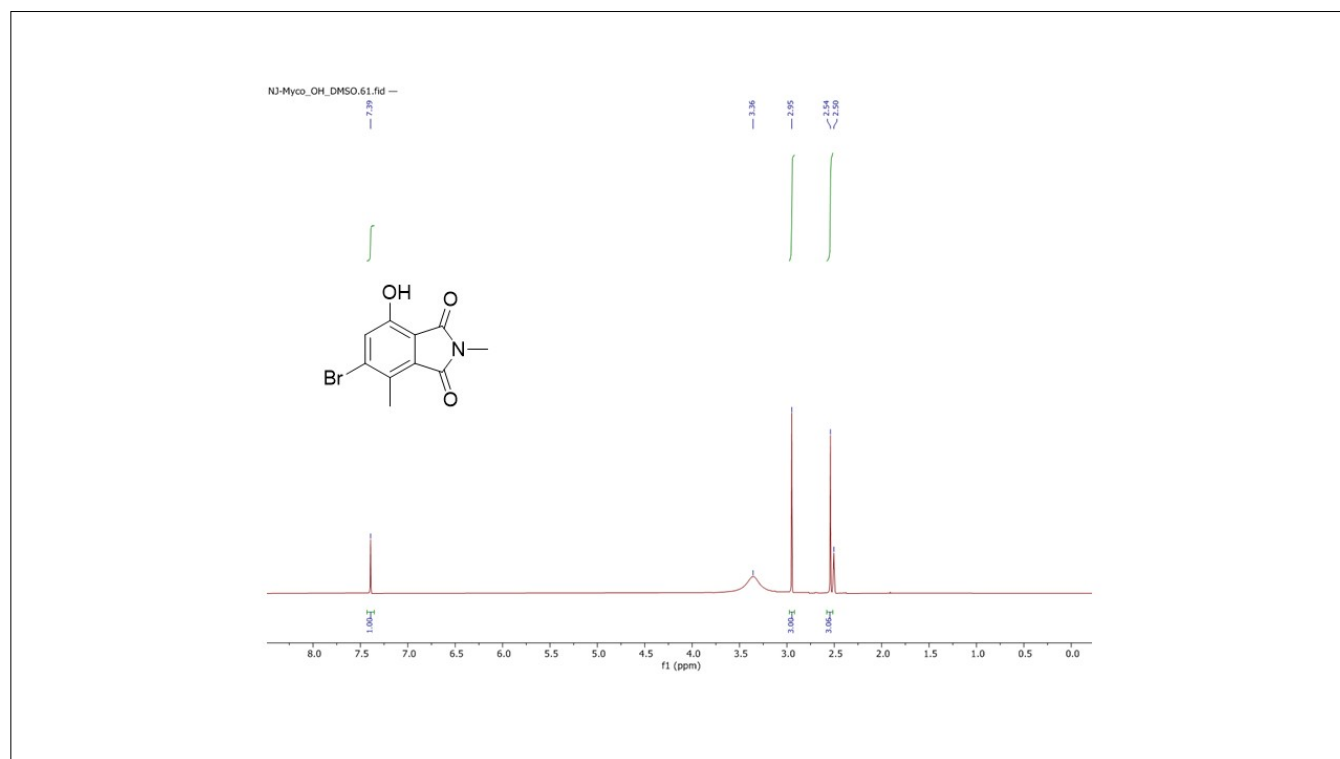
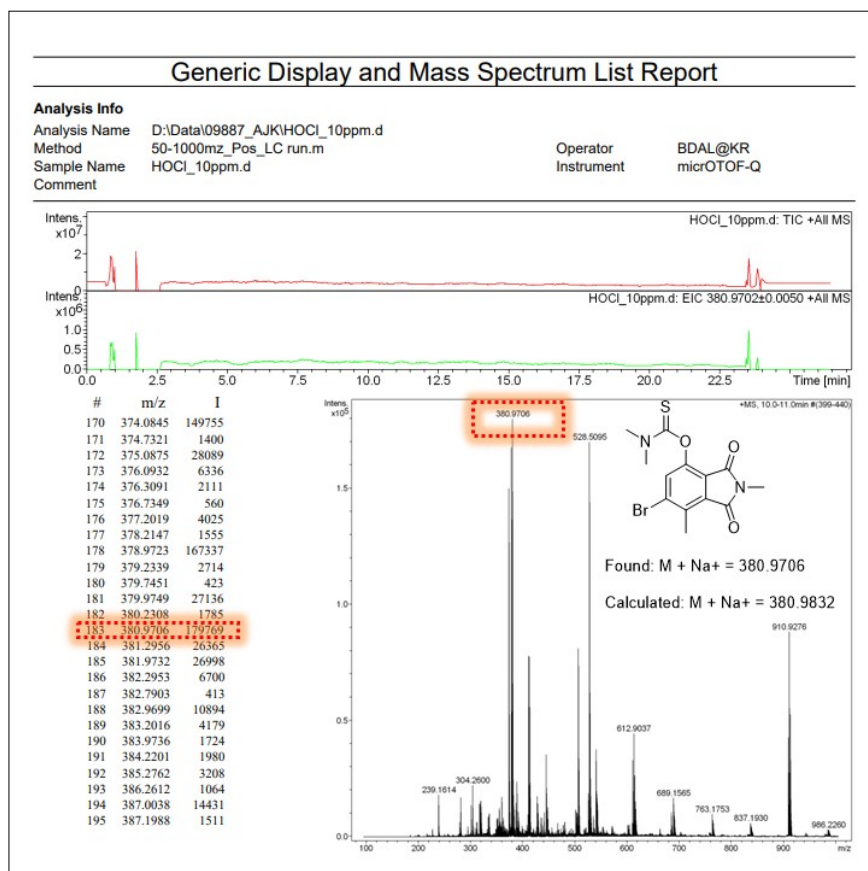


Fig. S7. HMBC spectrum of **Myco-OCl**.



**Fig. S8.**  $^1\text{H}$  NMR spectrum of **Myco-OH**.



**Fig. S9.** HR-MS (ESI) spectrum of **Myco-OCl**.

## Photophysical study:

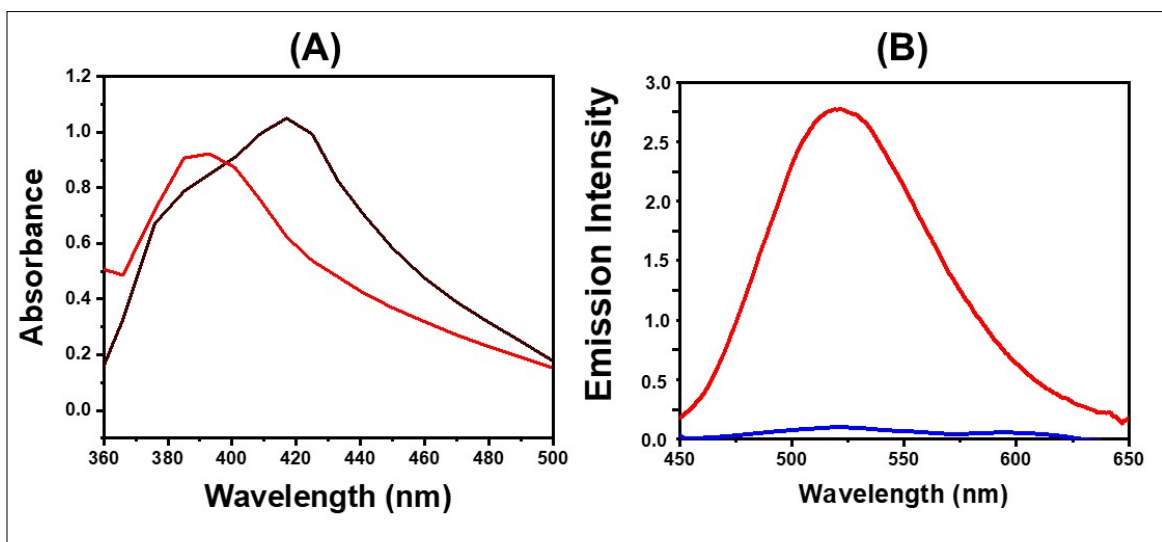


**Figure S10:** (A) Normalized UV- absorption spectra of **Myco-OCI** (10.0 μM) in absence (black) and presence (red) of HOCl (5 eq.) (B) Emission spectra of **Myco-OCI** (10.0 μM) in absence (black) and presence (red) of HOCl (0–50 μM) in the solution of PBS (10 mM, 7.4 pH) ( $\lambda_{\text{ex}} = 417 \text{ nm}$ ,  $\lambda_{\text{em}} = 522 \text{ nm}$ ; slit width = 5 nm/5 nm at RT).

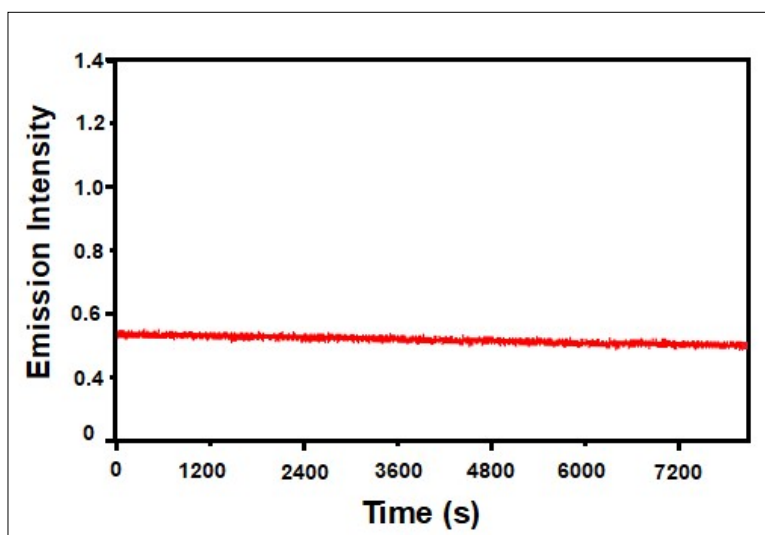


**Figure S11:** The time course of the fluorescence with the probe is shown supporting the photostability of **Myco-OCI** ( $\lambda_{\text{ex}} = 417 \text{ nm}$ ) without adding HOCl.

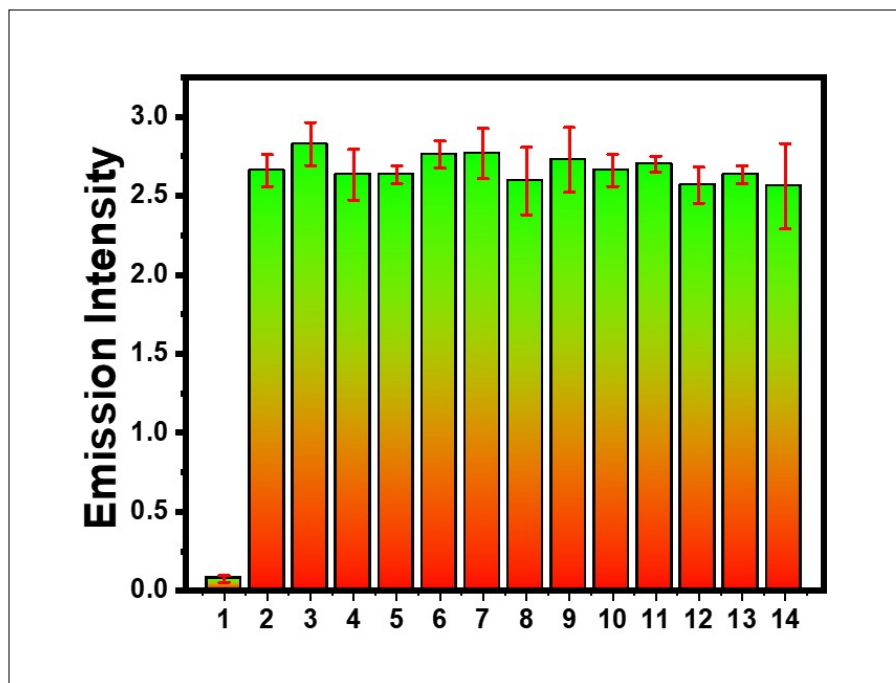


**Fig. S12.** Interference study of various ROS and bio thiols (100 equiv.) with **Myco-OCI** (10  $\mu\text{M}$ ) and HOCl (5 equiv) (1 to 14: = blank, HOCl,  $\text{O}_2^{\cdot-}$ , ONOO $^-$ ,  $\text{H}_2\text{O}_2$ ,  $^t\text{BuOOH}$ ,  $^i\text{BuOOH}$ , OH, NaHS, GSH, Cys, Hcy, ascorbic acid, and tyrosine respectively). ( $\lambda_{\text{ex}} = 417 \text{ nm}$  and  $\lambda_{\text{em}} = 522 \text{ nm}$ , slit width 5 nm / 5 nm). (Error bars are the average of three experiments).

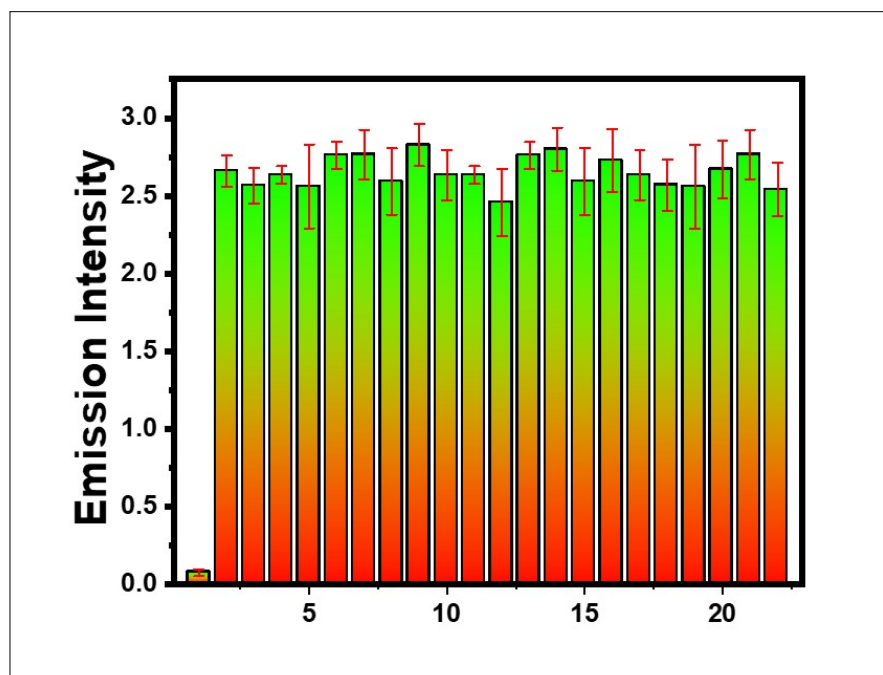


**Fig. S13.** Interference study of various metals and anions (100 equiv.) with **Myco-OCI** (10  $\mu\text{M}$ ) and HOCl (5 equiv) (1 to 22: = blank, HOCl,  $\text{K}^+$ ,  $\text{Na}^+$ ,  $\text{Ca}^{2+}$ ,  $\text{Mg}^{2+}$ ,  $\text{Pb}^{2+}$ ,  $\text{Mn}^{2+}$ ,  $\text{Zn}^{2+}$ ,  $\text{Cu}^{2+}$ ,  $\text{Fe}^{2+}$ ,  $\text{Fe}^{3+}$ ,  $\text{Mn}^{2+}$ ,  $\text{Cd}^{2+}$ ,  $\text{Al}^{3+}$ ,  $\text{Co}^{2+}$ ,  $\text{Cr}^{3+}$ ,  $\text{SO}_4^{2-}$ ,  $\text{S}_2\text{O}_3^{2-}$ ,  $\text{S}_2\text{O}_4^{2-}$ ,  $\text{S}_2\text{O}_5^{2-}$ , and  $\text{SO}_3^{2-}$  respectively ( $\lambda_{\text{ex}} = 417 \text{ nm}$  and  $\lambda_{\text{em}} = 522 \text{ nm}$ , slit width 5 nm / 5 nm). (Error bars are the average of three experiments).

## Cell imaging study:

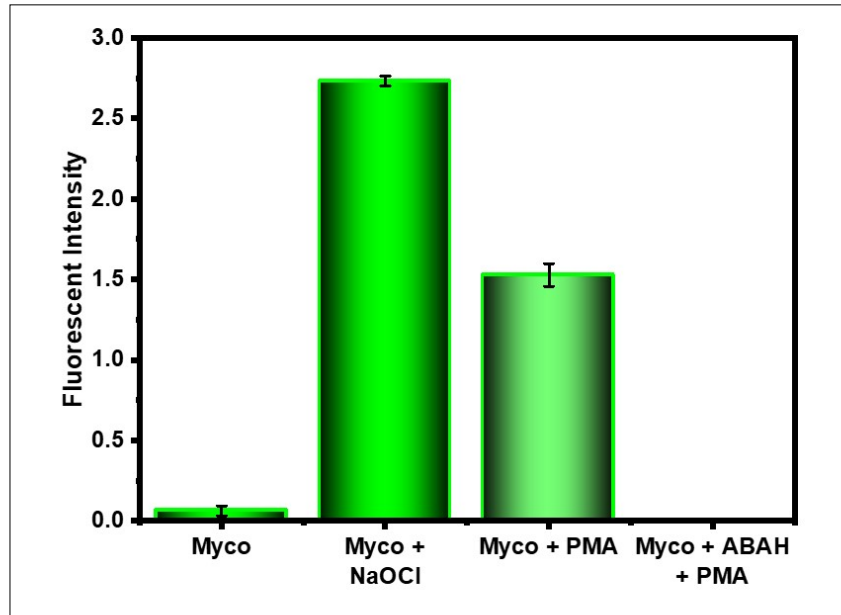


**Fig. S14.** Bar graphs showing the relative fluorescent intensities of the confocal microscopic images of A549 cells upon treatment with **Myco-OCI** (10  $\mu$ M), **Myco-OCI + NaOCl** (100  $\mu$ M), **Myco-OCI + PMA** (1  $\mu$ g mL<sup>-1</sup>), and **Myco-OCI + ABAH** (250  $\mu$ M) + **PMA** (1  $\mu$ g mL<sup>-1</sup>  $\mu$ M).

## Zebrafish imaging study:

### Animal Care (zebrafish):

Wild Type adult zebrafish were housed at 14/10 hour light/dark cycle at 28.5°C. Adult wild type and Tg(huc:egfp) were mated and embryos were collected and raised in E3 medium (5mM NaCl, 0.17mM KCl, 0.33mM CaCl<sub>2</sub>, 0.33mM MgSO<sub>4</sub>, 10-5% Methylene Blue) at 28.5°C. Proper developmental stages<sup>4</sup> were observed until experiments were conducted. All fish were obtained from the Zebrafish Center for Disease Modeling, Chungnam National University, Republic of Korea. All experiments were conducted according to the guidelines approved by the Animal Ethics Committee of Chungnam National University (CNU-0866).

### Chemical Treatment:

To identify the lethality of the Myco-OCI probe, 6dpf zebrafish were used. Four different concentrations (10, 20, 40, and 80 $\mu$ M) were prepared with 0.1% DMSO. Control (0.1% DMSO) was prepared separately. 6 dpf zebrafish larvae were exposed to control and four different concentrations in 24 well-plates and lethality was calculated using Kruskal Wallis One Way ANOVA post-test. Similarly, Tg(huc:egfp)



transgenic zebrafish lines were also exposed to four concentrations (10, 20, 30, 40  $\mu\text{M}$ ) to identify any abnormalities in neuronal development.

### Determination of morphological abnormalities:

Post 24-hour exposure, 7dpf zebrafish were analyzed for morphological abnormalities. We checked heartbeat rate, eye movement, eye size, pigment formation, pericardial edema, swim bladder development, and overall morphological defects. Similarly, *Tg(huc:egfp)* transgenic zebrafish were used to determine neuronal development in larval zebrafish. Each larva was then anesthetized using Tricaine (MS-222) and used for imaging.

### Animal Model Imaging:

7dpf zebrafish after verification for lethality was imaged under the MZ16 Brightfield microscope (Leica Biosystems, Wetzlar, Germany). 6dpf zebrafish fluorescent imaging was done with Logos Biosystems (Aligned Genetics, Republic of Korea).

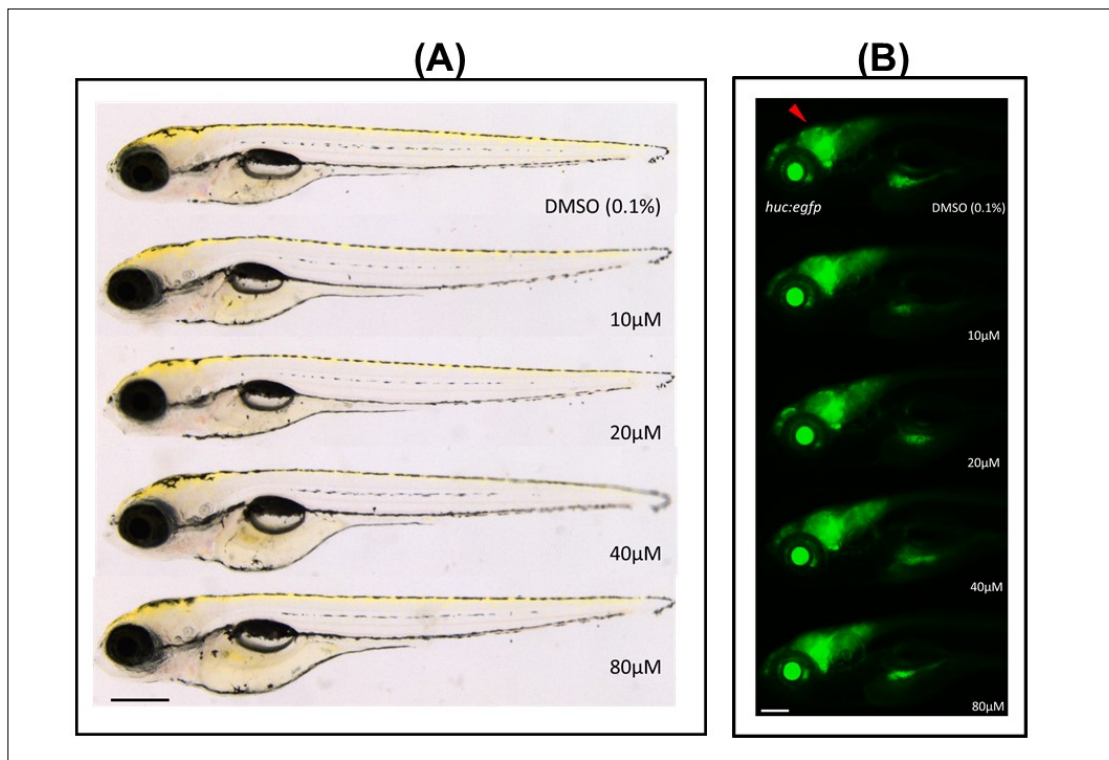


**Fig. S15.** (A) Investigation of morphological abnormalities of zebrafish larvae at 6dpf after 24h exposure to various concentrations (10, 20, 40, 80  $\mu\text{M}$ ) of **Myco-OCI probe**. (B) Effects of **Myco-OCI probe** with different concentrations (10  $\mu\text{M}$ , 20  $\mu\text{M}$ , 40  $\mu\text{M}$ , and 80  $\mu\text{M}$ ) on development of central nervous system in zebrafish larvae at 6 dpf. Fluorescent neurons are monitored in live transgenic zebrafish, *Tg(huc:gfp)*. The midbrain region is marked with red arrowheads. Signals in the intestine, yolk, and lens are due to autofluorescence.

References:

- 1 F. Tampieri, G. Cabrellon, A. Rossa, A. Barbon, E. Marotta and C. Paradisi, *ACS Sensors*, 2019, **4**, 3080–3083.
- 2 X. Lu, Z. Chen, X. Dong and W. Zhao, *ACS Sensors*, 2018, **3**, 59–64.
- 3 R. Yuan, Y. Ma, J. Du, F. Meng, J. Guo, M. Hong, Q. Yue, X. Li and C. Li, *Analytical Methods*, 2019, **11**, 1522–1529.
- 4 C. B. Kimmel, W. W. Ballard, S. R. Kimmel, B. Ullmann and T. F. Schilling, *Developmental Dynamics*, 1995, **203**, 253–310.